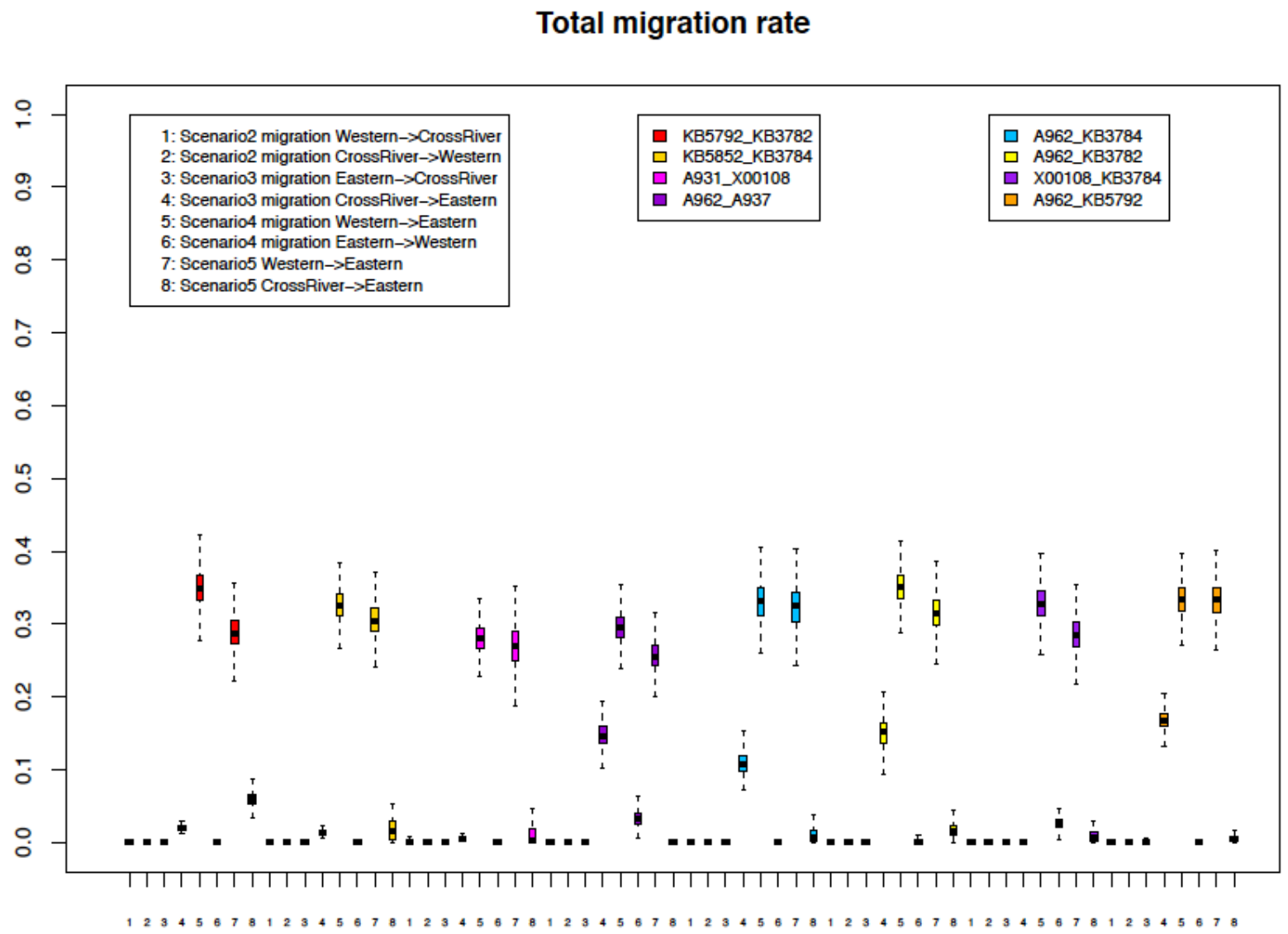

Figure S8: Total migration rate inferred by G-PhoCS, given by $m_{AB} * \tau_{AB}$.
Along the x-axis values from different migration bands associated with different scenarios (Figure 1) are depicted. The first six migration rate estimates come from a bi-directional migration setting. The last setting is with two migration bands, one from western lowland to eastern lowland gorilla and another from Cross River to eastern lowland gorilla. A strong signal of migration of western to eastern lowland gorillas is observed. Colors correspond to different combinations of western gorilla samples included in the analysis.

A.

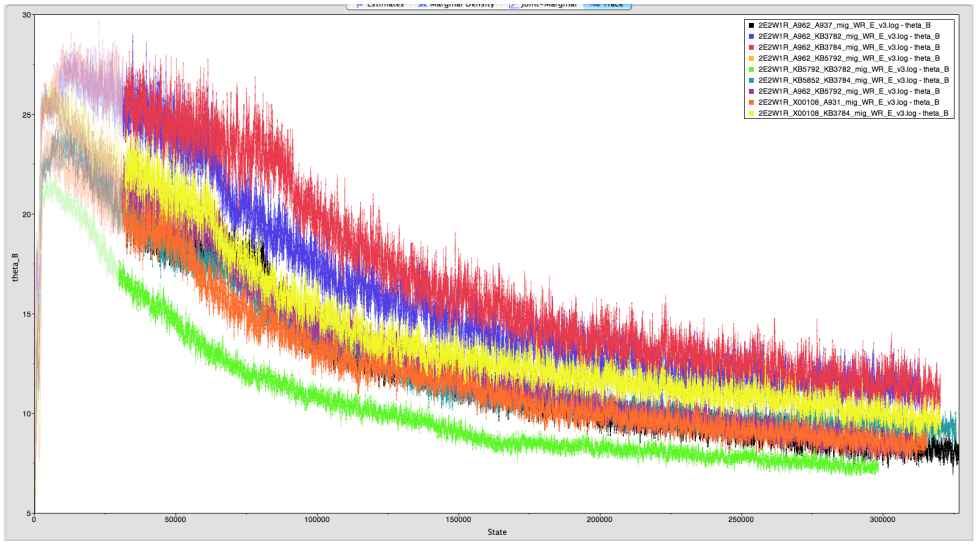
2E2W1R_A962_A937_mig_WR_E_v3.log - theta_B
2E2W1R_A962_KB3782_mig_WR_E_v3.log - theta_B
2E2W1R_A962_KB3784_mig_WR_E_v3.log - theta_B
2E2W1R_A962_KB5792_mig_WR_E_v3.log - theta_B
2E2W1R_KB5792_KB3782_mig_WR_E_v3.log - theta_B
2E2W1R_KB5852_KB3784_mig_WR_E_v3.log - theta_B
2E2W1R_A962_KB5792_mig_WR_E_v3.log - theta_B
2E2W1R_X00108_A931_mig_WR_E_v3.log - theta_B
2E2W1R_X00108_KB3784_mig_WR_E_v3.log - theta_B
theta_B
State

B.

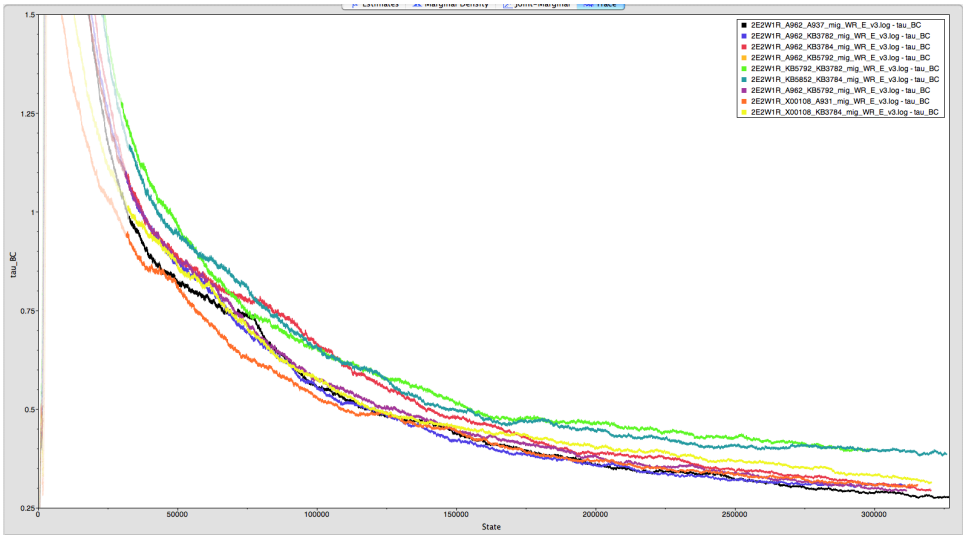
2E2W1R_A962_A937_mig_WR_E_v3.log - tau_BC
2E2W1R_A962_KB3782_mig_WR_E_v3.log - tau_BC
2E2W1R_A962_KB3784_mig_WR_E_v3.log - tau_BC
2E2W1R_A962_KB5792_mig_WR_E_v3.log - tau_BC
2E2W1R_KB5792_KB3782_mig_WR_E_v3.log - tau_BC
2E2W1R_KB5852_KB3784_mig_WR_E_v3.log - tau_BC
2E2W1R_A962_KB5792_mig_WR_E_v3.log - tau_BC
2E2W1R_X00108_A931_mig_WR_E_v3.log - tau_BC
2E2W1R_X00108_KB3784_mig_WR_E_v3.log - tau_BC
tau_BC
State

C.

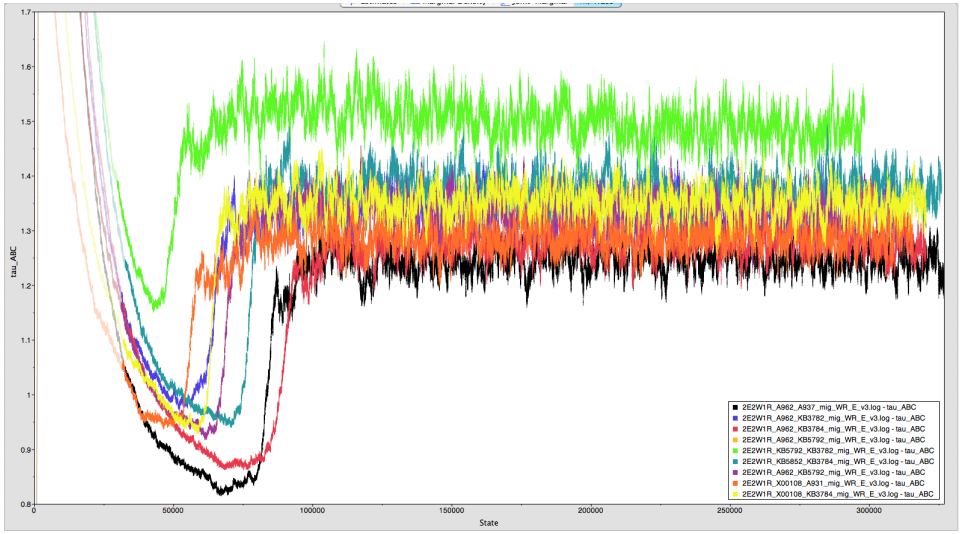

Figure S9: MCMC traces for three demographic parameters inferred using G-PhoCS.
Each trace plot (obtained using Tracer) displays 9 combinations of samples including 2 eastern gorillas, 2 western gorillas and 1 Cross River gorilla with migration setting scenario 5 (Figure 1). **A.** Western gorilla population size **B.** Western-Cross River gorilla split time **C.** Eastern-Western-Cross River ancestral split time

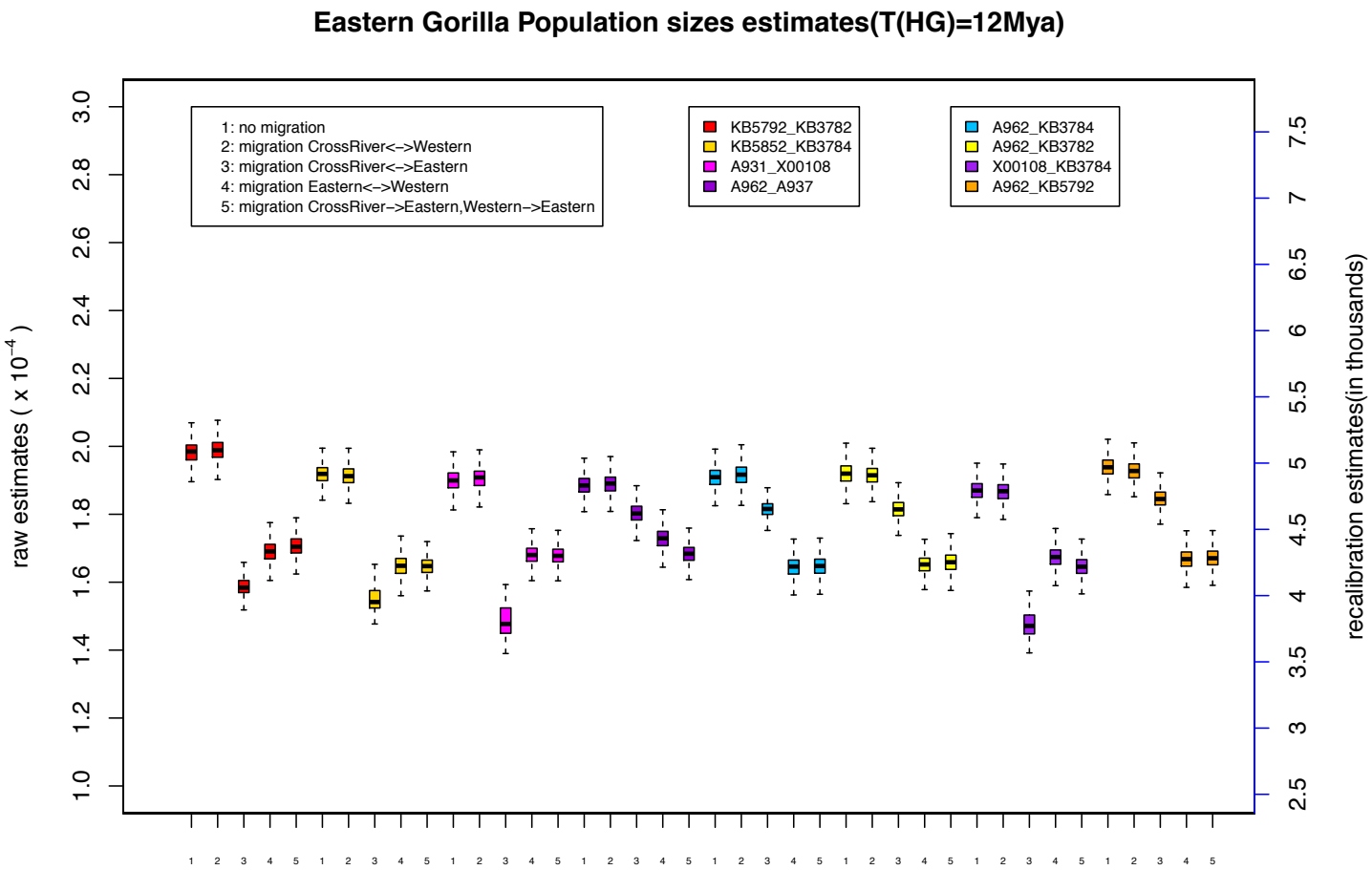

Figure S10: Eastern lowland gorilla population size estimates by G-PhoCS.
We include 2 eastern gorilla individuals (Victoria, 9732), different combinations of Western individuals, 1 Cross River gorilla (B646) and always include human reference as an outgroup. Values along the x-axis correspond to five different scenarios depicted in Figure 1. Raw estimates are depicted on the left axis scale, and recalibrated values (effective population size) assuming a human-gorilla divergence time of 12 Mya are depicted on the right axis.

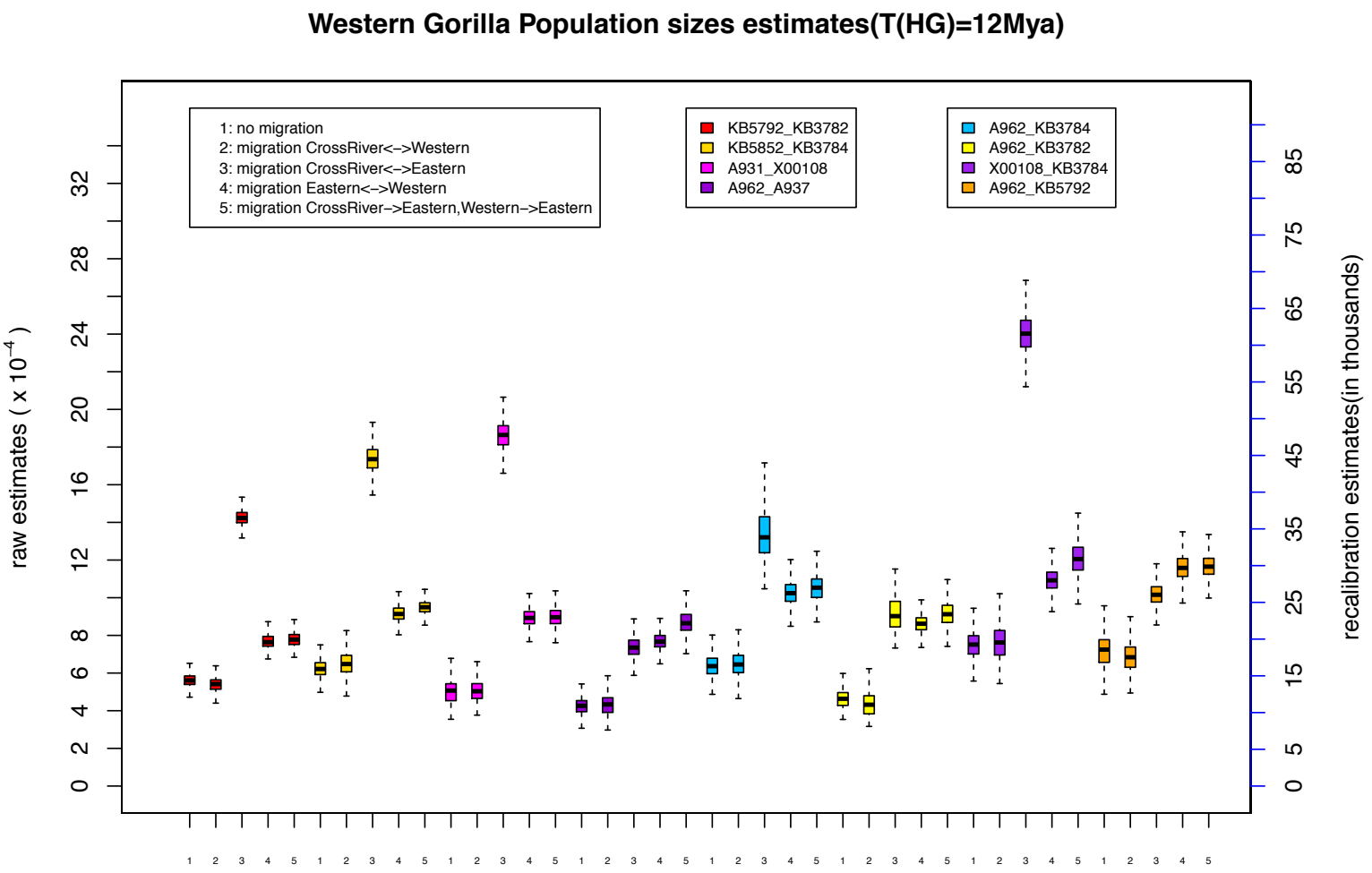

Figure S11: Western lowland gorilla population size estimates by G-PhoCS.
Values along the x-axis correspond to five different scenarios depicted in Figure 1. Raw estimates are depicted on the left axis scale, and recalibrated values (effective population size) assuming a human-gorilla divergence time of 12 Mya are depicted on the right axis.

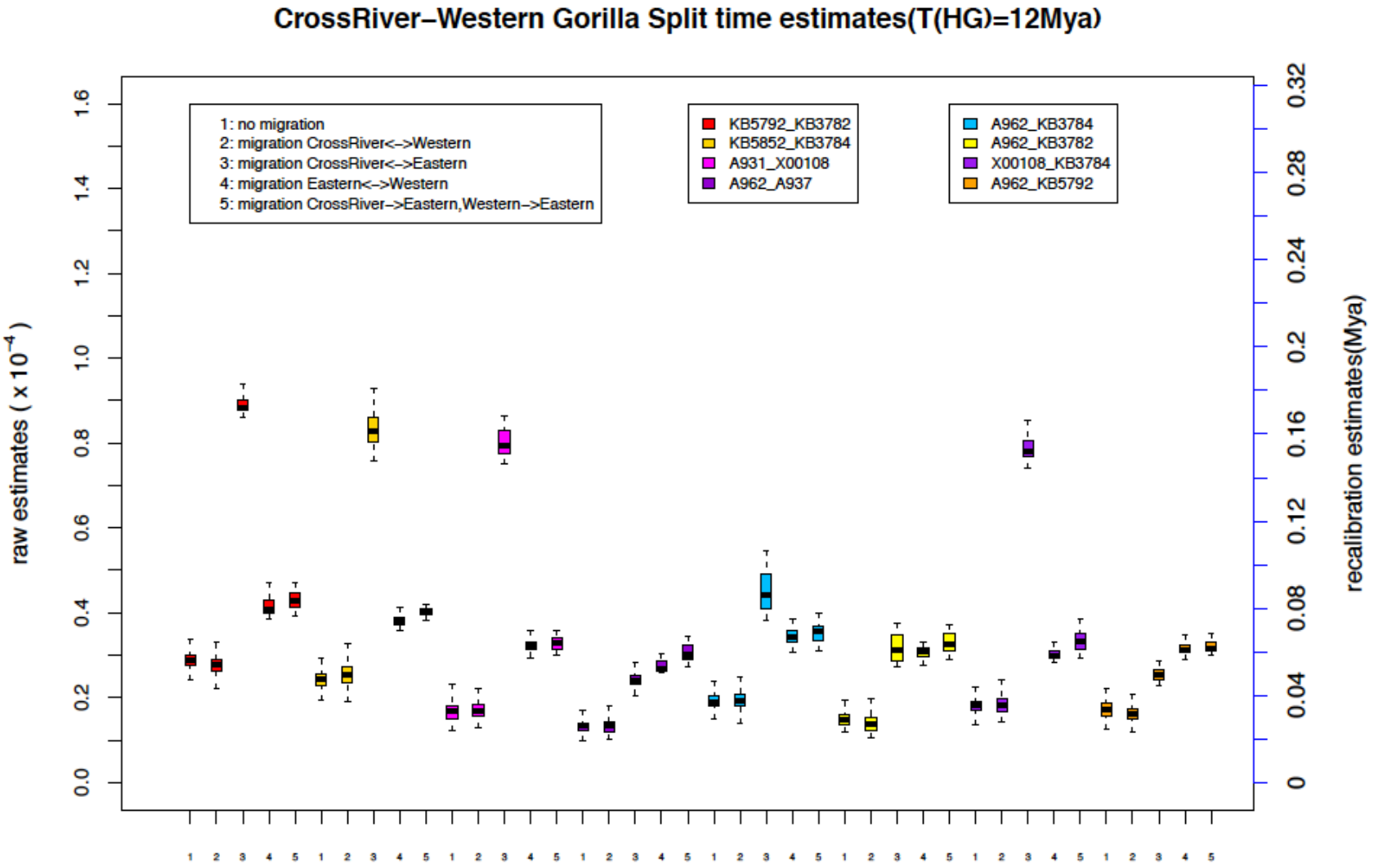

Figure S12: Western lowland and Cross River gorilla split-time estimates by G-PhoCS.
Values along the x-axis correspond to five different scenarios depicted in Figure 1. Raw estimates are depicted on the left axis scale, and recalibrated values assuming a human-gorilla divergence time of 12 Mya are depicted on the right axis.

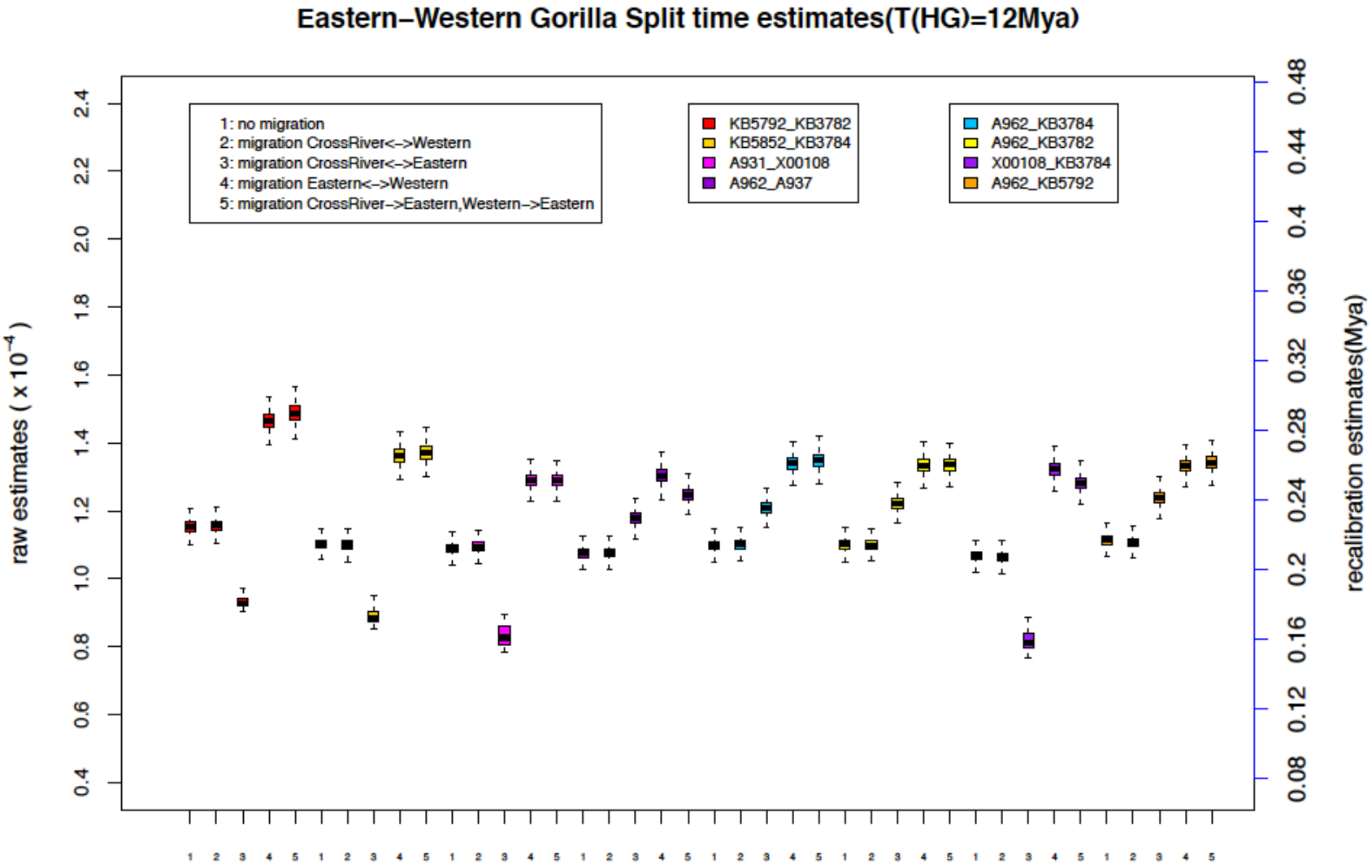

Figure S13: Eastern lowland and western-Cross River ancestral gorilla split-time estimates by G-PhoCS.
Raw estimates are depicted on the left axis scale, and recalibrated values (effective population size) assuming a human-gorilla divergence time of 12 Mya are depicted on the right axis.

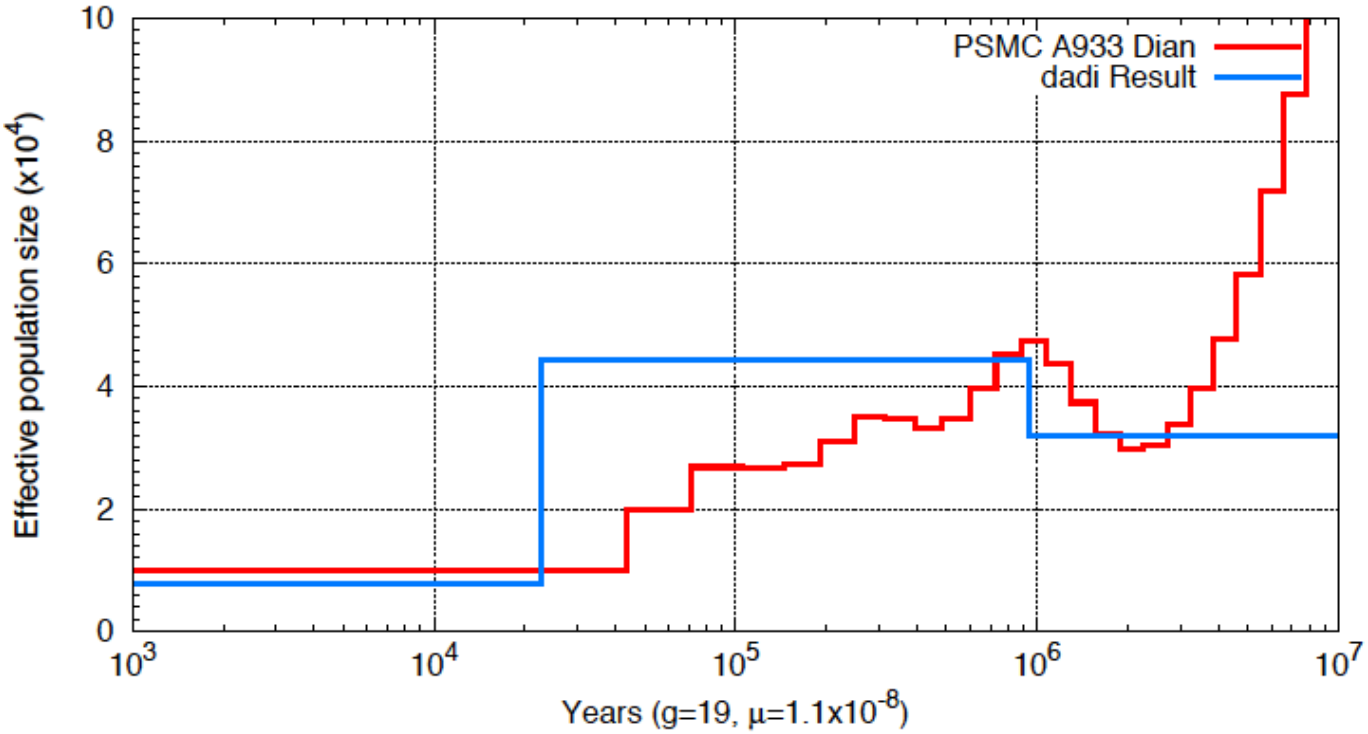

Figure S14: Comparison of *∂α∂i* and PSMC Models.
The red line indicates population history obtained for a western lowland gorilla using PSMC based on mapping to the gorilla genome and scaled using generation time and mutation rates employed in this paper. The blue line corresponds to the best-fit three-epoch model inferred for western lowland gorillas using *∂α∂i*.